Article

Experimental Study on Performance of Liquid–Gas Jet Pump with Square Nozzle

Xin Xu, Jiegang Mou *, Huiyan Zhang, Daohang Zou, Xuelong Yang *, Xiaohui Liu, Zhi Qiu and Buyu Dong

College of Metrology & Measurement Engineering, China Jiliang University, Hangzhou 310018, China; s21020804061@cjlu.edu.cn (X.X.); zhanghuiyan@cjlu.edu.cn (H.Z.); zoudaohang@cjlu.edu.cn (D.Z.); s21020408032@cjlu.edu.cn (X.L.); p21020854097@cjlu.edu.cn (Z.Q.); p21020854026@cjlu.edu.cn (B.D.)
* Correspondence: mjg@cjlu.edu.cn (J.M.); yxl@cjlu.edu.cn (X.Y.)

Abstract: An experimental study is conducted to investigate the effects of different operating parameters on the performance of liquid–gas jet pumps. A square nozzle with an area ratio of 2.25 is designed for the liquid–gas jet pump, and an experimental setup for the liquid–gas jet pump system is constructed. By varying parameters such as inlet flow rate, temperature, and inlet pressure, the variations in the pumping capacity and pumping ratio of the system are studied. The performance of liquid–gas jet pumps with square nozzles and traditional circular nozzles under the same working conditions was compared through experimental data. Explore the performance advantages and disadvantages of liquid–gas jet pumps with different shaped nozzles under the same working conditions. The experimental results indicate that as the inlet flow rate of the liquid–gas jet pump increases, the pumping capacity of the system increases, leading to an increase in the pumping ratio. The operational efficiency slightly decreases with a rise in the working water flow rate. The pumping ratio of the system increases with an increase in the inlet pressure, reaching a peak value of around 4.0 when the inlet valve is fully open. Inlet pressure significantly affects the efficiency of the liquid–gas jet pump, with the highest efficiency point achieved at Pa (inlet air pressure) = 60 kPa, reaching an operational efficiency of 42.48%. When Pa exceeds 70 kPa, the operational efficiency rapidly declines. Comparing the performance of square and circular nozzle liquid–gas jet pumps under the same operating conditions, the performance of the square nozzle liquid–gas jet pump outperforms that of the circular nozzle counterpart. The pumping system's performance decreases continuously with an increase in the working liquid temperature; however, the decline in pumping performance becomes gradual after exceeding 40 °C. As the water level rises, both the pumping capacity and pumping ratio of the system increase. After the liquid level reaches 40 cm, the changes in the pumping system's performance become less pronounced.

Keywords: liquid–gas jet pump; square nozzle; pumping performance; performance studies

1. Introduction

Jet pump design theory has a history of over 100 years of research. As a type of fluid conveyance machinery and a mixing and reaction device, jet pumps are widely used in conjunction with other pumping systems, finding extensive applications in agriculture, water conservancy, transportation, and other fields [1].

Hoeffer [2] conducted successful extraction experiments using liquid–gas jet pumps in condensers for the first time. Then, through extensive experimental studies, Rammingen [3] discovered that the pressure of two-phase fluids suddenly increased after mixing. Witte [4], through experimental research, discovered that in the process of water and gas mixing within the liquid–gas jet pump, the gas undergoes significant compression, greatly impacting the pump's performance. A dimensionless constant (Euler number) was introduced to elucidate the complex two-phase flow during the liquid–gas mixing process, defining what a mixing shockwave is. Betzler [5] primarily conducted experimental studies on the

diffuser structure. The results showed that optimal suction efficiency of the liquid–gas jet pump is achieved when the gas and liquid phases are already mixed within the throat section. Subsequently, an overall structural optimization study was carried out on the liquid–gas jet pump, revealing a correlation between the isothermal compression ratio of air and the throat length-to-diameter ratio. The optimal isothermal compression ratio of air occurs at a throat length-to-diameter ratio of 22, approximately 18%. Opletal [6] studied the influence of the geometric parameters of the jet pump on the injection ratio and mass transfer coefficient, showed that the working structure parameters had an important influence on the injection performance of the LGJP and proposed a method to evaluate the mass transfer performance. Winoto [7] conducted experimental research on the correlation between the conditions of maximum flow rate in liquid–gas jet pumps and the suction and discharge pressures. The results showed that solely reducing the suction pressure does not lead to an earlier occurrence of the maximum flow rate. However, under lower inlet pressure conditions, further reducing the discharge pressure causes the maximum flow rate to occur earlier. The liquid–gas jet pump remains operationally stable at the state of maximum flow rate, and visualization of the throat section revealed that the mixing foam is already formed before the maximum flow rate state is reached.

Cunningham [8], through an extensive analysis of experimental results, suggested that under optimal conditions, as long as appropriate values for the throat length-to-diameter ratio and throat diameter are chosen in the structure of liquid–gas jet pumps, the isothermal compression ratio of air can exceed 40%, and possibly even higher. This finding provides reference for the structural design in this study. Additionally, Witte [4] employed a 19-nozzle multi-jet structure and conducted experimental comparisons under various operating conditions, ultimately achieving an isothermal compression ratio of 40%. Kumar [9] applied liquid–gas jet pumps to seawater purification systems and conducted related experimental research. The results indicated that the pump's performance reached an optimum value when the nozzle-to-throat entrance distance was 33 mm. Furthermore, the relationship between nozzle diameter, throat-to-nozzle distance, area ratio, and the performance of liquid–gas jet pumps was studied through experiments by Kumar et al., and these theoretical results were validated, showing good agreement between experimental and theoretical outcomes. Bo Hu [10], studied the flow characteristics within the pre-swirl system of a marine gas turbine at low rotational speed by varying the pressure at the pre-swirl nozzle. Ge Qiang [11] designed the structural parameters of liquid–gas jet pumps and developed calculation programs using VB and Access databases for the pump's structural dimensions. Additionally, CFD (Computational Fluid Dynamics) software was utilized for numerical simulation analysis of the mixing process of two-phase fluids within the liquid–gas jet pump under different structural parameters. The results showed that when operating efficiency reaches its maximum, the throat-to-nozzle distance should be 1.5 times the nozzle diameter, and the nozzle throat area ratio (m) should be 5.86, resulting in an efficiency of 0.232.

Eisallak [12] conducted experimental analysis of the impact of inlet pressure on jet streams. The results showed that when the inlet pressure is relatively weak, the performance of the liquid–gas jet pump improves, while with higher inlet pressure, the pump's efficiency decreases. Xiang Qingjiang [13] conducted pressure measurements on the diffuser wall under different gas-liquid volume flow rate ratios. Experimental results indicated that within the diffuser, the maximum pressure increment ranged up to 250 kPa, with pressure initially decreasing and then increasing along the wall. Consequently, the installation of the liquid–gas jet pump should consider the pressure changes within the diffuser caused by the static pressure resulting from vertical height. Zhang [14] summarized the design theory, internal flow mechanism, structural optimization, and practical applications of liquid–gas jet pumps, with a particular focus on discussing pulse liquid–gas jet pumps. Yandong Gu [15] analyzed the performance degradation of the multi-stage centrifugal pump and optimized the performance and axial forces. Cheng Honggui [16], in order to study the flow characteristics of ultra-large area ratio jet pumps, performed numerical

simulations and structural optimizations on jet pumps with different area ratios. The results showed that as the flow ratio increased, the resistance of the entrained fluid increased rapidly. Unlike conventional jet pumps, the pressure ratio exhibited a parabolic decline, and the point of highest efficiency shifted to the right as the area ratio increased. Haidl [17] used a converging nozzle to measure the suction capacity of a conventional liquid–gas jet pump while experimenting with the performance of the pump in less stable configurations, providing the best design suggestions for units with various geometric shapes, directions and operating conditions to minimize gas entrainment.

Yang Xuelong [18] used the orthogonal experimental design method to design the jet pump's throat length, diffuser angle and profile, and analyzed three parameters to obtain the optimal combination of throat and diffuser tubes. Hui Qianglong [19] conducted an experimental study on the performance of liquid–gas jet pumps with several special-shaped nozzles. The results showed that when the area is relatively large, the maximum liquid–gas ratio of the liquid–gas jet pump formed by the special-shaped nozzles is greater than that of circular nozzles. He Weidong [20] and colleagues conducted an experimental study to verify the impact of jet pump supply liquid temperature on the energy-saving effectiveness of a plate freezer. Performance experiments were carried out at four different temperatures: 25, 30, 35, and 40 °C. The results indicated that the performance of the plate freezer initially increased and then decreased as the condensation temperature rose. This suggests that the working fluid temperature affects the efficiency of the jet pump, thereby influencing the overall system efficiency. In order to improve the performance of the jet pump. The above research shows that the pumping efficiency of the liquid–gas jet pump is affected by the internal structure of the liquid–gas jet pump and external parameter conditions such as temperature. This paper studies the factors affecting the external performance of square nozzle liquid–gas injection pumps, exploring the effects of different parameters on the performance of the experimental system of the square nozzle liquid–gas jet pump. The paper establishes an experimental platform for the liquid–gas jet pump system to investigate the effects of these three influencing factors on the system's performance. This includes using a controlled variable method to verify the impact of factors such as inlet flow rate, inlet pressure, and inlet water temperature during the operation of the liquid–gas jet pump system. Additionally, a comparison is made between the efficiency changes of square nozzle and traditional circular nozzle liquid–gas jet pumps under the same area ratio. Different air inlet pressure and water inlet flow parameters have a greater impact on the efficiency of the liquid–gas jet pump. The square nozzle with the same area ratio has better efficiency and performance under different parameter conditions.

2. Experimental Apparatus Design

2.1. Experimental Setup and Instruments

Design and construct the experimental platform framework for the liquid–gas jet pump system according to experimental requirements, and establish the experimental procedure as shown in Figure 1.

Based on the design diagram of the pump system experimental platform, the experimental setup of the system was constructed, as shown in Figure 2. The liquid–gas jet pump system experimental platform consists of a working pump (liquid–gas jet pump), a pressurization pump (centrifugal pump), a motor, pipeline valves, performance acquisition equipment, and other relevant components. The system is driven by the electric motor (13), and the working fluid is discharged from the water tank (1), pressurized through the centrifugal pump (2), and its flow is controlled by a valve installed on the working pipe [21]. The flow rate of the working fluid is measured by flowmeter (4). The fluid then enters the liquid–gas jet pump (6) through the pipeline (5). Gas enters through the inlet (8), passes through the inlet pipe (9) and the float flowmeter (10), and is controlled by the inlet valve (11). The gas is mixed with the working fluid in the pressure-stabilizing tank (12), and the mixed liquid is passed through the diffuser pipe (7) before being discharged back into the water tank for recycling.
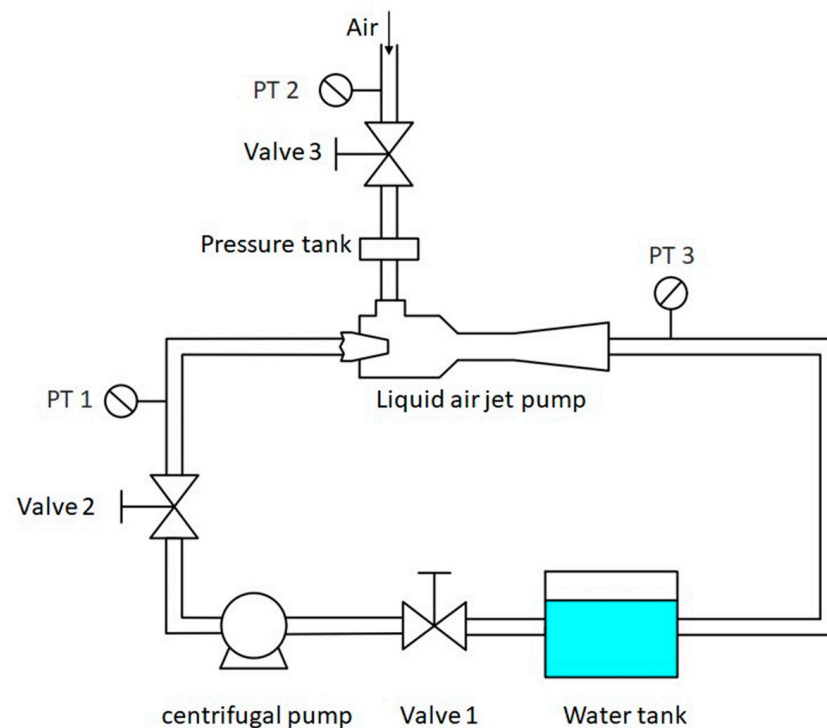
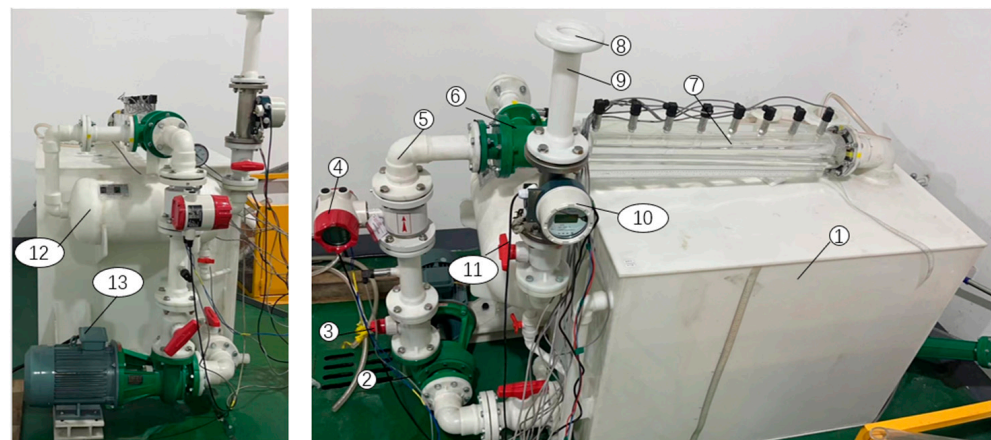**Figure 1.** Design drawing of the pump system experimental platform.

Figure 2. Physical diagram of the pump system experimental platform. 1—Water tank, 2—Centrifugal pump, 3—Inlet valve, 4—Flowmeter, 5—Inlet pipeline, 6—Liquid–gas jet pump, 7—Diffuser pipe, 8—Inlet port, 9—Inlet pipe, 10—Float flowmeter, 11—Inlet valve, 12—Pressure-stabilizing tank, 13—Motor.

2.2. Device Parameters

The centrifugal pump in this experimental setup is employed as a pressurization pump. The chosen pump operating performance parameters to meet the requirements are as follows: rated flow rate (Q_n) of 50 m³/h, rated head (H_m) of 32 m, rated rotational speed frequency (f_n) of 50 Hz, and it is matched with a motor of 7.5 kW power.

For the working pump of this system (liquid–gas jet pump), the design will involve adjusting certain dimensional parameters based on a comparison between practical operational needs and theoretical analysis. The structure of the liquid–gas jet pump is depicted in Figure 3, and the structural parameters are detailed in Table 1.
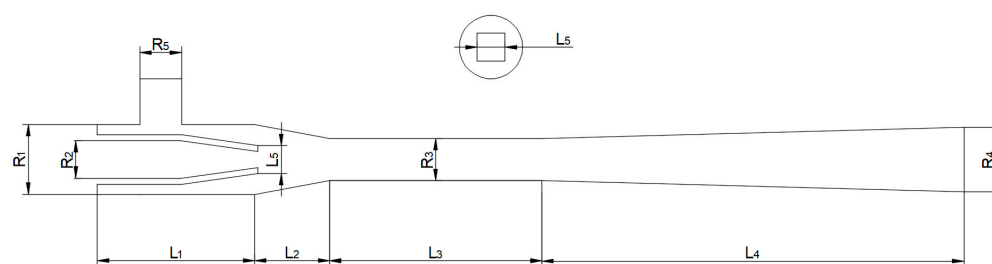
Figure 3. Structure diagram of the liquid–gas jet pump.

Table 1. Structural parameters of the liquid–gas jet pump.

Main Structure	Dimensions
Suction chamber length (L_1)	250 mm
Mixing chamber length (L_2)	120 mm
Throat length (L_3)	370 mm
Diffuser length (L_4)	630 mm
Nozzle side length (L_5)	78 mm
Suction chamber inner diameter (R_1)	110 mm
Inlet port inner diameter (R_2)	65 mm
Throat inner diameter (R_3)	66 mm
Diffuser outlet inner diameter (R_4)	100 mm
Inlet port inner diameter (R_6)	65 mm
Area ratio (m)	2.25

The working fluid inlet pressure of the liquid–gas jet pump is generally around 0.6 MPa. The pressurization pump is used to increase the water pressure inside the water tank to 0.6 MPa. The gas directly connected to the atmosphere is drawn into the system through the inlet pipeline at a pressure of 0.1 MPa. The pressure variation range at the outlet of the mixed fluid is 0.1–0.25 MPa.

The air pumping volume (Q_a) and inlet water pressure (P_a) are among the most crucial performance indicators. Therefore, the fluid flow entering through the inlet valve or inlet gas valve is controlled, and the water pressure is measured using a pressure transmitter.

2.3. Performance Indicators of Liquid–Gas Jet Pump

In order to provide a better understanding of the relationship between the operational performance of the liquid–gas jet pump and the flow characteristics of the internal two-phase liquid–gas flow, this study employs dimensionless numbers such as the volume flow rate ratio (q) and the working efficiency (η) and area ratio (m) of the liquid–gas jet pump to describe its performance. These performance indicators offer an intuitive reflection of the mass and energy transfer processes within the liquid–gas jet pump:

(1)　Volume Flow Rate Ratio (q) [22].

$$q = \frac{Q_a}{Q_g} \tag{1}$$

In the equation,

Q_a stands for the air pumping volume;
Q_g stands for the inlet water flow.

(2)　Area Ratio (m) [23].

$$m = \frac{f_b}{f_o} \tag{2}$$

f_b represents the throat cross-sectional area;
f_o represents the nozzle cross-sectional area.

(3)　　Working Efficiency (η) [22].

Unlike liquid–liquid jet pumps, the fluid movement inside a liquid–gas jet pump involves gas compression and changes in density, making it impossible to use the efficiency formula of liquid–liquid jet pumps for calculation. The working efficiency of a liquid–gas jet pump is essentially the ratio of the energy gained by the pumped gas to the energy lost by the working fluid.

The gas is drawn into the liquid–gas jet pump through the inlet port and then mixed with the jetting liquid before exiting through the outlet. This process can be visualized as an isothermal compression process.

The energy gained by the gas is given by the following equation:

$$W_a = \int_{v_a}^{v_c} p \, dv = \int_{v_a}^{v_c} \frac{p_a v_a}{v_x} d(v_x) = p_a v_a \ln\left(\frac{v_c}{v_a}\right) \tag{3}$$

In the equation,

v_a represents the velocity of the gas entering the liquid–gas jet pump;
v_x is the gas velocity along the axis of the liquid–gas jet pump;
v_c is the velocity at which the gas leaves the liquid–gas jet pump.

According to the ideal gas equation:

$$pv = nRT \tag{4}$$

In the equation,

p represents pressure;
v represents the volume of the gas;
n represents the amount of substance of the gas;
R is the molar gas constant;
T stands for temperature.

As the gas is assumed to undergo an isothermal compression process, the temperature T remains constant, and the gas medium does not change. Therefore, the following derivation can be conducted:

$$W_a = p_a v_a \ln\left(\frac{v_c}{v_a}\right) = p_a v_a \ln\left(\frac{p_a}{p_c}\right) \tag{5}$$

The energy loss of the working fluid is:

$$W_g = Q_g \Delta p \tag{6}$$

In the equation, Δp represents the total pressure difference lost by the liquid from entering the liquid–gas jet pump to leaving it.

Therefore, the expression formula for working efficiency is:

$$\eta = \frac{W_a}{W_g} \tag{7}$$

3. Experimental Design

In order to investigate the effects of various factors on the performance of the liquid–gas jet pump system, experiments with controlled variables of different parameters were conducted on the experimental platform of the liquid–gas jet pump system. The aim was to delve into the influence of parameter variations on the performance of the pump system. This study examines the factors that may affect the operating conditions of the pump system through experiments and generates corresponding performance curves.

The pump parameters were adjusted to operate the pump within a highly efficient and stable working range. The operating point of the pump corresponds to the intersection

of the pump performance curve and the pipeline curve. Altering the operating point of the pump is referred to as pump regulation. When the pump's model is fixed, its performance curve remains constant. Thus, adjusting the operating point of the pump intelligently involves modifying various parameters of the operating system. Changing the system's performance curve can be achieved by adjusting factors such as inlet pressure, intake pressure, friction losses, and local losses. Friction losses and local losses are closely related to components within the system, such as pipe diameter, roughness, angles, and more. Due to experimental limitations, altering pipe parameters is not possible; therefore, the operating point of the liquid–gas jet pump system is primarily regulated by adjusting inlet flow rate, intake pressure, and working fluid temperature.

3.1. Experimental Design with Inlet Flow Rate as the Single Variable

Ensure all valves are in the closed position. Start the centrifugal pump motor and allow it to run until it reaches a stable state. Slowly adjust the gas valve and the inlet water valve to fully open positions. Record data from various sensors, including inlet flow rate and intake pressure. Subsequently, gradually adjust the inlet water valve opening, recording experimental data at 5 m^3/h intervals while simultaneously adjusting the gas valve to maintain a stable intake pressure.

After the liquid–gas jet pump has been running stably for 2 min, continuously collect sensor data for 60 s. Gradually adjust the inlet water valve until the working water flow rate is insufficient to maintain continuous gas suction. Throughout this process, maintain the water flow rate as the sole variable while adjusting the gas valve to keep the intake pressure constant. Upon completion of data collection, first adjust the gas valve to fully open and then stop the motor to prevent backflow and ensure that liquid does not enter the pressure-stabilization tank.

3.2. Experimental Design with Inlet Pressure as the Single Variable

Ensure all valves are closed. Start the centrifugal pump motor and wait for the centrifugal pump to reach a stable operating state. Gradually adjust the gas valve and inlet water valve to fully open positions. Record data from all sensors. Subsequently, gradually reduce the valve opening in increments of 10 kPa, recording experimental data at each interval. Simultaneously adjust the inlet water valve to maintain a stable working water flow rate. Similarly, after the liquid–gas jet pump system has run stably for 2 min, continuously collect sensor data for 60 s. Gradually adjust the gas valve until the jet of liquid is no longer able to sustain stable gas suction. Throughout this process, maintain the inlet pressure as the sole variable, adjusting the inlet water valve to keep the working water flow rate constant. After completing the data collection, first fully open the gas valve. Then, stop the motor to prevent backflow and the entry of liquid into the pressure-stabilization tank.

3.3. Experimental Design with Inlet Water Temperature as a Single Variable

In practical engineering, the temperature of the liquid can be influenced by weather and working conditions, causing fluctuations in the working fluid's temperature. Since the design temperature of the liquid–gas pump in the system is 15 °C, the system can operate normally when the mixed liquid temperature of the cooling water for the pump and the steam extracted from the condenser is below 20 °C. During the summer, environmental temperatures often exceed 30 °C, and the efficiency of the liquid–gas pump drops significantly when the working fluid temperature exceeds 30 °C, resulting in a much lower pumping capacity than the design value. When the variation in inlet water temperature exceeds a certain range, it affects the performance of the liquid–gas pump system, preventing the system from maintaining efficient and stable operation. To investigate the effect of inlet water temperature on the experiment, the experimental setup on the test bench was used, maintaining a constant motor speed of 1800 rpm while varying the inlet water temperature and recording experimental data. In this process, the inlet air pressure was kept as the only

variable. Based on the experimental data, performance curves for the liquid–gas pump system at different inlet water temperatures were plotted.

4. Experimental Validation

In Figure 4, In the operational conditions of the system, changes in valve opening affect the inlet flow rate and inlet air pressure. Therefore, adjustments to the inlet flow rate and inlet air pressure can be achieved by controlling the valve opening. The valve opening of the pipeline valves influences the pumping performance curve of the pump system. By controlling and maintaining the valve opening within a reasonable range, the liquid–gas pump system can operate stably and efficiently in the working area over the long term. Experiments were conducted using the constructed experimental setup, keeping the electric motor's speed constant at 1800 rpm. Different valve openings were manually adjusted, and experimental data were recorded. Based on the experimental results, performance curves for this liquid–gas pump system were plotted at various valve openings.
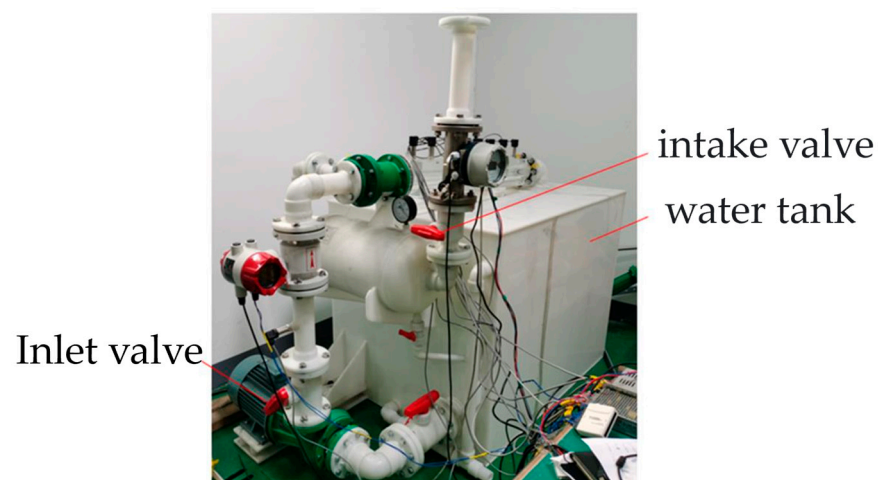

Figure 4. The specific location of different parameters.

During the experimental process, measurement errors are unavoidable. Factors such as vibrations caused by the centrifugal pump can affect the accuracy of sensors, especially the sensitivity of the float-type flowmeter. Additionally, significant measurement deviations can occur due to the impact of liquid droplets on the pressure taps in the throat and diffuser tubes. To ensure the credibility and accuracy of the experimental data, it is necessary to conduct error analysis and correction on the collected data. Pressure transducers, float-type flowmeters, and electromagnetic flowmeters have a high data acquisition frequency of up to 1000 Hz. The data collection process generates a large volume of data, and significant errors may arise due to uncontrollable factors such as vibrations. To address this, error correction is performed on the experimental data using the 3-sigma rule.

The criterion, assuming a sufficiently large number of measurements and an adequate amount of data, is based on the assumption that only random errors exist in the data. It involves calculating the standard deviation from the data and setting a range interval around this standard deviation value. Any data points outside of this range are considered gross errors and should be removed.

The 3σ criterion, assuming a sufficiently large number of measurements and an adequate amount of data, presupposes that only random errors exist in the data. After calculating and processing the data, the standard deviation value is determined. A range interval is established around this deviation value, and data points falling outside this interval are considered gross errors and should be removed. When performing precision measurements on the object under test, independent measurements $x_1, x_2 \ldots x_n$, are obtained. The arithmetic mean x and the residual errors $v_i = x_i - x$ ($i = 1, 2, \ldots n$) are calculated. The standard deviation σ is then computed using Bessel's formula. If the

residual error v_b ($1 \leq b \leq n$) of a specific measurement value x_b satisfies the following condition, the data point x_b is considered to be a gross error and it is removed from the dataset:

$$|v_b| = |x_b - x| > 3\sigma \tag{8}$$

After removal, the average of the remaining data is taken as the measured data for this group of data.

Since the intake airflow measurement point and the intake pressure measurement point in the experimental setup designed in this paper are not located at the same position, there are pressure changes and heat exchange when the extracted gas enters the pressure-stabilizing tank. Therefore, there is a difference between the collected intake airflow and the actual flow at the intake pressure measurement point. During the gas movement in the pipes and the pressure-stabilizing tank, there is no heat exchange with the surroundings, and it is considered an adiabatic process. According to Poisson's law equation:

$$P \times V^Y = C \tag{9}$$

In the equation, *P* represents gas pressure, *V* represents volume, *Y* represents specific heat ratio, and *C* represents a constant.

The gas flowmeter employs a float-type flowmeter, and its measurement data are the gas flow rate at 20 °C and 4 kPa gas pressure. The measurement environment is maintained at 20 °C. By substituting these values into the Poisson's law equation, the accurate actual gas flow rate at the intake pressure measurement point is obtained.

4.1. Impact of Inlet Flow Rate Results

The variation in inlet flow rate is primarily controlled by the valve opening. The flow rate of the working fluid pumped by the centrifugal pump depends on the valve opening, and changes in the valve opening are used to alter the working fluid flow rate. Experiments were conducted under controlled conditions, meaning that other variables were kept constant. The experimental inlet water temperature was set at 20 °C, the water tank liquid level was maintained at 70 cm, and the inlet valve opening was adjusted as necessary to maintain an inlet pressure of around 90 kPa. The experimental setup was started, and data collection was initiated, once the system reached a stable operational state. The experimental results are presented in the curves shown in Figures 5 and 6.
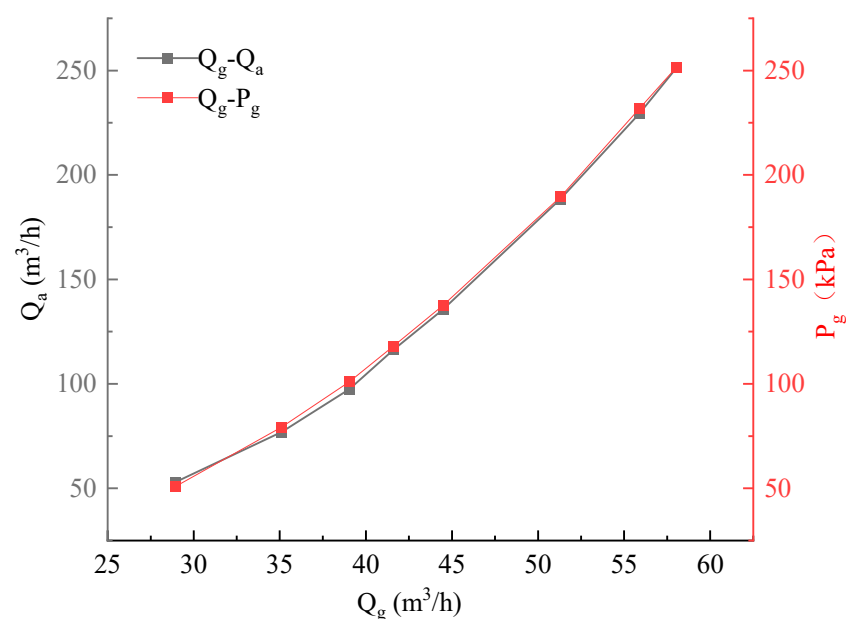

Figure 5. Changes in air extraction rate with different inlet flow rates.
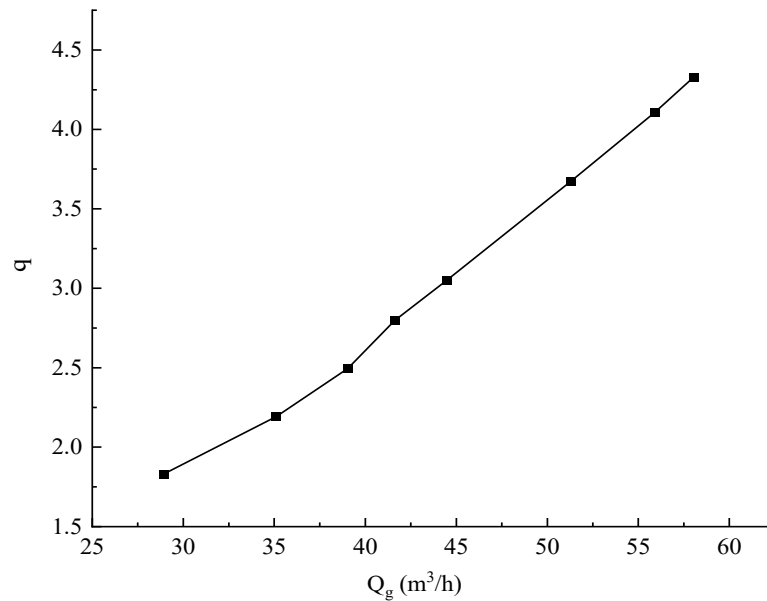
Figure 6. Changes in air extraction ratio with different inlet flow rates.

From Figures 5 and 6, it can be concluded that as the inlet flow rate of the working fluid increases, both the pumping capacity and pumping efficiency of the liquid–gas pump system also increase. As shown in Figure 7, it can be observed that the efficiency slightly decreases with an increase in the working fluid flow rate, but the impact is limited, with the maximum efficiency variation reaching only 9.17%.
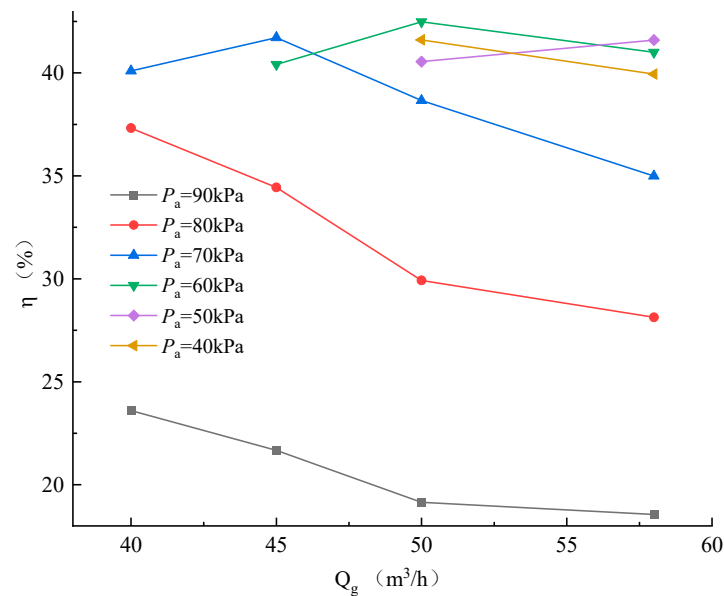

Figure 7. Impact of the inlet water flow rate on efficiency.

4.2. Impact of Inlet Pressure Results

The gas flow extracted by the liquid–gas pump is primarily controlled by the inlet valve. Changes in the experimental gas flow rate are achieved by altering the valve opening. Experiments were conducted under controlled conditions, with the experimental inlet water temperature held at 20 °C and the water tank liquid level at 70 cm. By varying the inlet valve opening and adjusting the inlet water valve to maintain a constant inlet water flow rate of 58 m^3/h, the experimental results are presented in the curves shown in Figures 8 and 9.
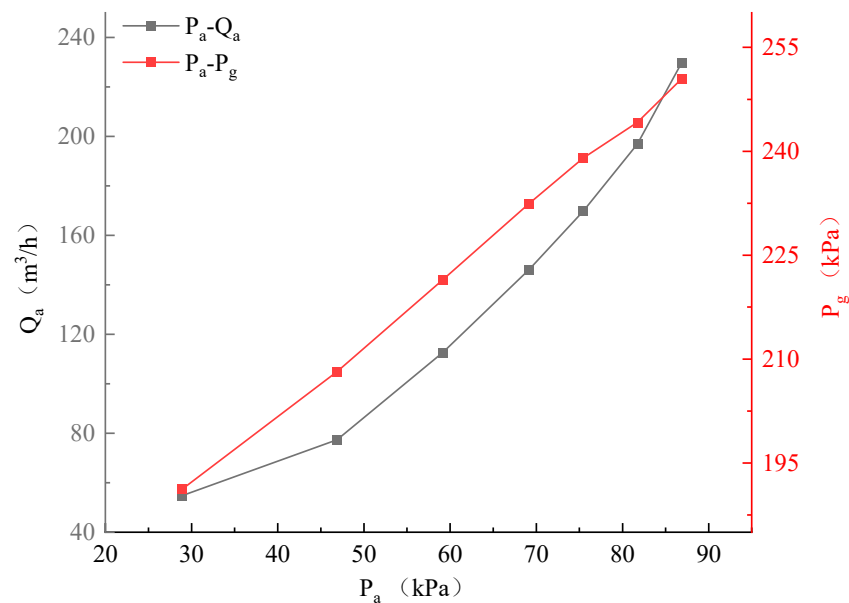
Figure 8. Changes in air extraction rate with different inlet pressure levels.
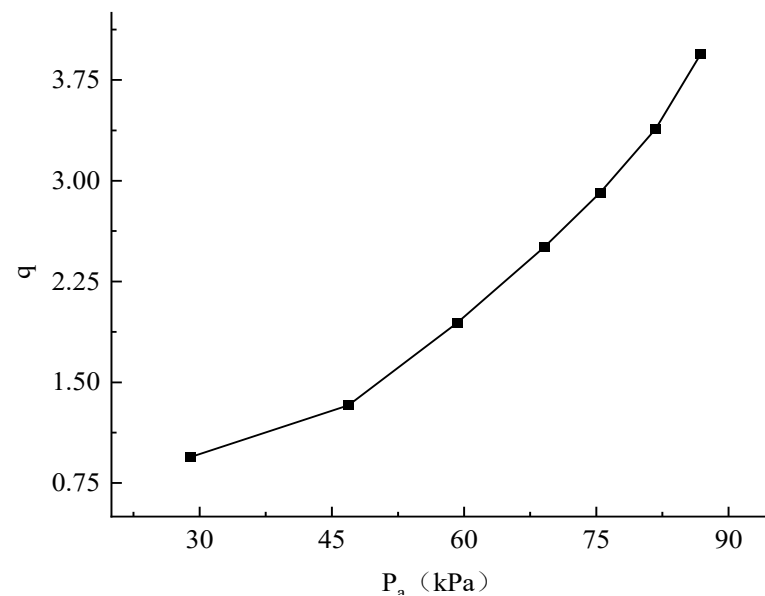

Figure 9. Changes in air extraction ratio with different inlet pressure levels.

From Figures 8 and 9, it is evident that keeping the inlet water pressure constant while changing the inlet pressure results in corresponding variations in the pumping performance of the liquid–gas pump system. As the inlet pressure increases, both the pumping capacity and pumping efficiency of the system also increase. When the inlet valve is fully open, the pumping efficiency reaches a peak of around 4.0.

Figure 10 shows that the inlet pressure has a significant impact on the efficiency of the liquid–gas pump. The working efficiency is relatively high and stable when Pa is less than or equal to 70 kPa. However, when Pa exceeds 70 kPa, the working efficiency decreases rapidly. The highest efficiency point is observed at Pa = 60 kPa, with a working efficiency of 42.48%.
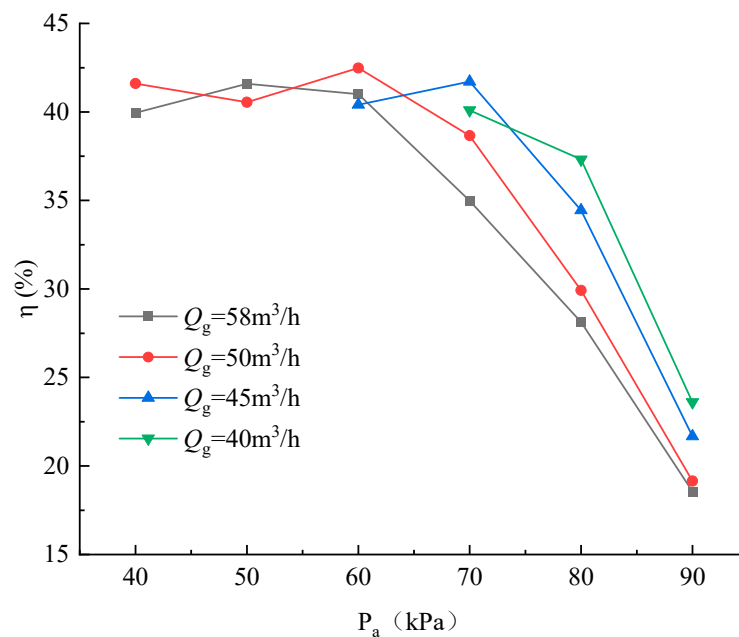
Figure 10. Influence of inlet pressure on efficiency.

According to the literature reference [24], the area ratio (m) of circular nozzles in liquid–gas pumps ranges from 1.96 to 7.92. Efficiency gradually increases and then decreases within this range, as shown in Figure 11. However, there is a trend of increasing efficiency when the area ratio is between 2 and 3. The efficiency curves in the figure are all plotted based on the maximum efficiency corresponding to the area ratio.
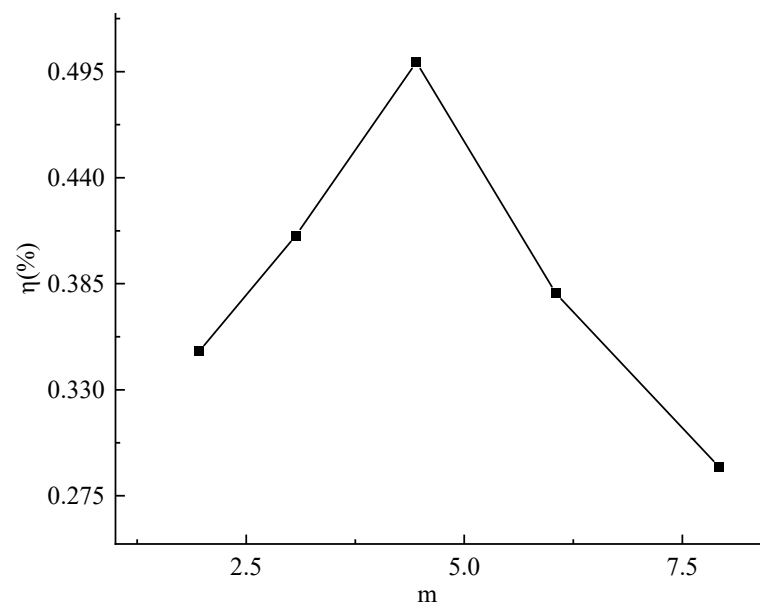

Figure 11. Efficiency curves of jet pump for different area ratios.

According to Table 2 in the literature, the optimal efficiencies for area ratios of 1.96 and 3.07 in jet pumps are 0.35 and 0.41, respectively. Based on the trend in the curves, it can be observed that the efficiency of a circular nozzle liquid–gas pump with an area ratio of 2.25 falls between 0.35 and 0.40. In contrast, the square nozzle liquid–gas pump in this study achieves an optimal efficiency of 42.48% with an area ratio of 2.25. This indicates that for the same area ratio, the square nozzle configuration outperforms traditional circular nozzles in terms of working efficiency.

Table 2. Working parameters of the pump system at different temperatures.

| T (°C)	P_g (kPa)	P_a (kPa)	Q_a (m³/h)	Q_g (m³/h)
15	252.715	90.118	253.706	58.252
20	252.22	89.966	251.07	58.179
25	251.692	90.174	243.798	57.983
30	251.7045	90.446	244.476	58.089
35	251.028	90.096	237.793	58.185
40	249.644	90.782	230.952	58.27
45	250.437	91.075	230.574	58.384

4.3. Impact of Inlet Water Temperature Results

Experiments were conducted under controlled conditions, with the water tank liquid level maintained at 70 cm. The inlet water temperature (T) was gradually increased from 15 to 45 °C, with increments of 5 °C each time. Table 2 presents experimental data for the liquid–gas pump system's pumping performance at different inlet water temperatures while keeping both the inlet water and inlet air valves fully open and achieving maximum working efficiency.

From the table above, it can be observed that in the liquid-ring gas jet pump system with the inlet water and inlet air valves fully open, the water-pumping capacity of the system remains almost constant, consistently at around 58 m³/h. However, the gas-pumping capacity gradually decreases with the increase in inlet water temperature. Figures 12 and 13 depict the changes in gas-pumping capacity and gas-pumping ratio of the pump system as the water temperature rises.

From the above figure, it can be seen that with the inlet water and inlet air valves fully open and all other conditions remaining constant, the overall liquid-ring gas jet pump system gradually decreases as the inlet water temperature rises. However, when the inlet water temperature exceeds 40 °C, the gas-pumping ratio changes more gradually within the temperature range of 40–45 °C.

At different water temperatures, while maintaining the system's inlet air pressure at 90 kPa, the inlet water pressure was varied. Figure 14 illustrates the overall gas-pumping performance of the liquid-ring gas jet pump system at different temperatures.
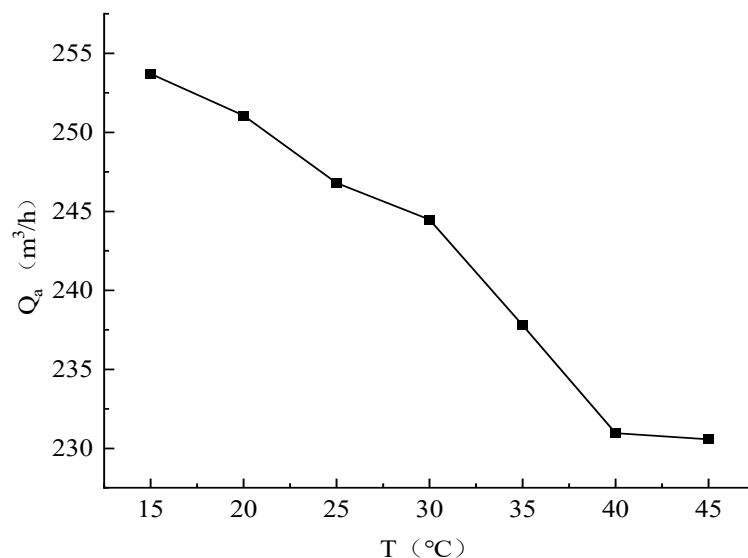
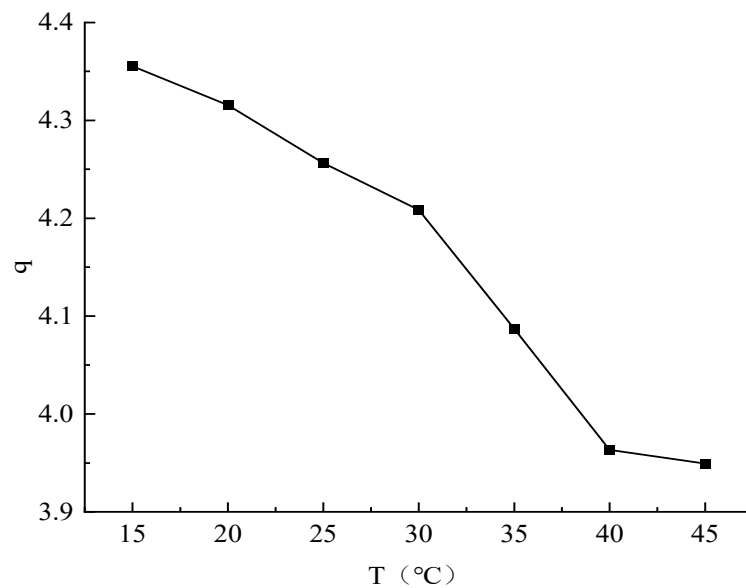**Figure 12.** Changes in air extraction rate at different inlet water temperatures.

Figure 13. Changes in air extraction ratio at different inlet water temperatures.
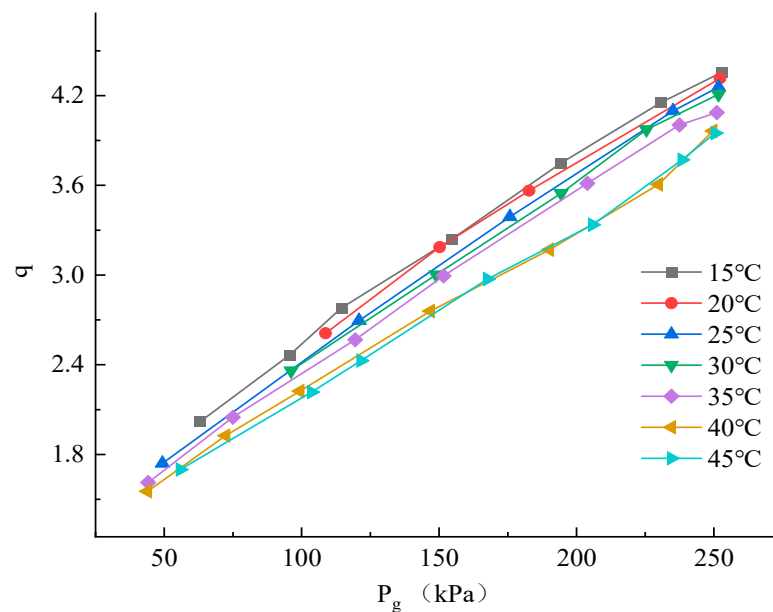

Figure 14. Changes in air extraction ratio with varying inlet pressure at different temperatures.

From the above Figure 14, it can be observed that at the same inlet water pressure, the gas-pumping performance of the liquid-ring gas jet pump system gradually decreases as the inlet water temperature increases. At a constant temperature, the system's gas-pumping performance increases with an increase in inlet water pressure, and the performance curve of the system approximately shifts with the same slope to the lower right. The most significant change in the system's gas-pumping performance occurs in the temperature range of 35 to 40 °C. When the water temperature exceeds 40 °C and is within the 40–45 °C temperature range, the change in gas-pumping ratio of the liquid-ring gas jet pump system is not significant, and the gas-pumping ratio curves of the system almost overlap.

At different inlet water temperatures, with a constant inlet water flow rate of 58 m^3/h, the inlet air pressure was varied to conduct a gas-pumping performance test on the liquid-ring gas jet pump system. The following Figure 15 illustrates the changes in the overall gas-pumping performance of the system at different temperatures for comparison.
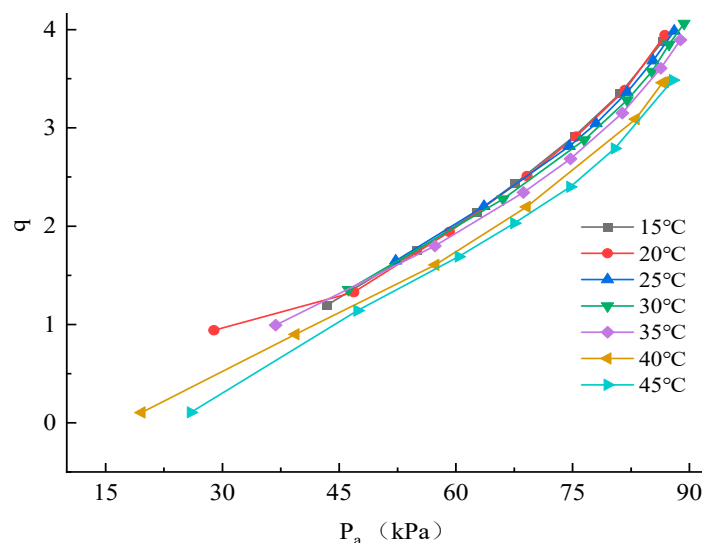
Figure 15. Changes in the air-to-fuel ratio with varying intake pressure at different temperatures.

From the above Figure 15, it can be observed that the gas-pumping performance of the liquid-ring gas jet pump system continuously decreases as the inlet water temperature increases. When the inlet water temperature varies within the range of 15–30 °C, the gas-pumping performance of the liquid-ring gas jet pump system remains relatively stable, and the curves approximate each other. However, when the inlet water temperature changes in the range of 35–45 °C, the gas-pumping performance of the liquid-ring gas jet pump system varies significantly, and the system's gas-pumping curve noticeably shifts to the lower right.

5. Conclusions

This study conducted experimental research on various parameters affecting the performance of the liquid-ring gas jet pump system using a controlled variable approach. Performance curves of the liquid-ring gas jet pump system were plotted, and the gas-pumping efficiency of the system was observed by analyzing the trends in these curves. Based on this, the following conclusions can be drawn:

(1) Under the condition of keeping other factors constant, the air extraction efficiency of the liquid–gas jet vacuum pump system increases with an increase in the water inflow rate. Simultaneously, under the condition of maintaining other variables consistent, the liquid–gas jet vacuum pump system exhibits an increase in air extraction efficiency with an increase in the air intake pressure. Therefore, this verifies that the water inflow rate and air intake pressure have a significant impact on the performance of the liquid–gas jet vacuum pump system.

(2) Keeping other conditions constant while adjusting the water temperature, the air extraction efficiency of the liquid–gas jet pump system decreases as the water temperature rises. Within the temperature range of 35–40 °C for the water inflow, the air extraction performance undergoes the most significant changes. However, once the water temperature exceeds 40 °C, the liquid–gas jet vacuum pump system's air extraction performance remains relatively stable. This experiment segment confirms the significant impact of water temperature on the performance of the liquid–gas jet vacuum pump system.

(3) When the area ratio is the same and equal to 2.25, changing the inlet water flow or air inlet pressure of the liquid-vapor jet pump system, it was found that the square nozzle liquid-ring gas jet pump exhibits higher operational efficiency than the circular nozzle counterpart. Under this specific area ratio, the square nozzle liquid-ring gas jet pump system demonstrates superior performance.

(4) Performance experiments were conducted on the liquid–gas jet pump system, exploring the factors leading to changes in its performance. Additionally, a comparison was made between the performance of nozzles with different shapes but the same area ratio. This research provides a basis for enhancing the performance of liquid–gas jet pumps and related areas.

Author Contributions: Conceptualization, J.M., H.Z., D.Z., X.Y., X.L., Z.Q. and B.D.; Methodology, X.X.; Writing—original draft, X.X. All authors have read and agreed to the published version of the manuscript.

Data Availability Statement: Data are contained within the article.

Conflicts of Interest: The authors declare no conflict of interest.

Nomenclature

P_a the inlet air pressure, m^3/h
P_g the inlet water pressure, kpa
Q_g the inlet water flow, m^3/h
Q_a the air pumping volume, m^3/h
q the volume flow rate ratio
m the area ratio
T the inlet water temperature, °C

References

1. Wu, J.; Yuan, D.Q.; Wang, G.J.; Liu, J.C. Current Situation and Prospect of Jet Pumps. *J. Drain. Irrig. Mach. Eng.* **2007**, *25*, 65–68.
2. Neve, R.S. The performance and modeling of liquid jet gas pumps. *Int. J. Heat Fluid Flow* **1988**, *9*, 156–164. [CrossRef]
3. Kumar, R.S.; Kumaraswamy, S.; Mani, A. Experimental investigations on a two-phase jet pump used in desalination systems. *Desalination* **2007**, *204*, 437–447. [CrossRef]
4. Witte, J.H. Mixing Shocks and Their Influence on the Design of Liquid–Gas Ejectors. Ph.D. Thesis, Delft University, Delft, The Netherlands, 1962.
5. Betzler, R.L. The Liquid–Gas Jet Pump Analysis and Experimental Results. Ph.D. Thesis, Pennsylvania State University, State College, PA, USA, 1969.
6. Opletal, M.; Novotný, P.; Linek, V.; Moucha, T.; Kordač, M. Gas suction and mass transfer in gas-liquid up-flow ejector loop reactors. Effect of nozzle and ejector geometry. *Chem. Eng. J.* **2018**, *353*, 436–452. [CrossRef]
7. Winoto, S.H.; Shah, D.A.; Li, H. Visualization in Water Jet Pump Throat under Limiting Flow Condition. *J. Flow Vis. Image Process.* **1998**, *5*, 78–83. [CrossRef]
8. Cunningham, R.G. Liquid jet pumps for two-phase flows. *J. Fluids Eng.* **1995**, *117*, 309–316. [CrossRef]
9. Kumar, R.S.; Mani, A.; Kumaraswamy, S. Analysis of a jet-pump-assisted vacuum desalination system using power plant waste heat. *Desalination* **2005**, *179*, 345–354. [CrossRef]
10. Hu, B.; Yao, Y.; Wang, M. Flow and Performance of the Disk Cavity of a Marine Gas Turbine at Varying Nozzle Pressure and Low Rotation Speeds: A Numerical Investigation. *Machines* **2023**, *11*, 68. [CrossRef]
11. Ge, Y.J.; Ge, Q.; Yang, J. Numerical Simulation and Confirming of Optimal Range on the Nozzle-to-throat Clearance of Liquid–gas Jet Pump. *Fluid Mach.* **2012**, *40*, 21–24.
12. Mikheev, N.I.; Davletshin, I.A.; Mikheev, A.N.; Kratirov, D.V.; Fafurin, V.A. Efficiency of liquid-jet high-pressure booste compressors. *J. Phys. Conf. Ser.* **2017**, *891*, 012202. [CrossRef]
13. Xiang, Q.J.; Wu, Y.L. Experimental study on flow in diffuser of liquid-jet gas pump. *J. Drain. Irrig. Mach. Eng.* **2014**, *32*, 558–562.
14. Zhang, H.Y.; Zou, D.H.; Yang, X.L. Liquid–Gas Jet Pump: A Review. *Energies* **2022**, *15*, 6978. [CrossRef]
15. Gu, Y.; Sun, H.; Wang, C. Effect of Trimmed Rear Shroud on Performance and Axial Thrust of Multi-Stage Centrifugal Pump with Emphasis on Visualizing Flow Losses. *J. Fluid Eng.* **2024**, *146*, 11. [CrossRef]
16. Cheng, H.G.; Long, X.P.; Yang, X.L. Numerical Simulation and Flow Analysis of Performance for Ultra-Large Area Ratio Jet Pumps. *Fluid Mach.* **2012**, *40*, 38–41.
17. Haidl, J.; Mařík, K.; Moucha, T.; Rejl, F.J.; Valenz, L.; Zednikova, M. Hydraulic characteristics of liquid–gas pump with a coherent liquid jet. *Chem. Eng. Res. Des.* **2021**, *168*, 435–442. [CrossRef]
18. Yang, X.L.; Long, X.P. Effects of diffuser structure and throat length on jet pump performance. *J. Harbin Inst. Technol.* **2014**, *46*, 111–115.

19. Hun, Q.L.; Xiang, Q.J.; Li, H. Experimental Study on the Performance of Liquid Jet Gas Pump with Non-circular Nozzle. *Fluid Mach.* **2011**, *39*, 1–4, 16. [CrossRef]
20. He, W.D.; Wan, J.Q.; Ge, R. Experimental Study on Plate Freezer with Two-Phase Ejector. *J. Eng. Therm. Energy Power* **2019**, *34*, 111–115.
21. Li, M.Q.; Chen, Y.L.; Hua, Y.M. Experimental study on liquid jet pump based on cyclic symmetrical aeration. *J. Drain. Irrig. Mach. Eng.* **2022**, *40*, 223–229. [CrossRef]
22. Wang, Y.L. Study on Characteristics of Liquid Gas Jet Pump. Master's Thesis, Taiyuan University of Technology, Taiyuan, China, 2015.
23. Xiang, Q.J.; Yun, Q.L.; Li, H. Experiment Study on Hydraulic Performance of Liquid Jet Gas Pump with Wide Range of Area Ratio. *Fluid Mach.* **2012**, *40*, 1–5.
24. Xing, R. Three-Dimensional Simulation of Liquid–Gas Jet Pump for Evaluating Vacuum. Master's Thesis, Shandong University, Jinan, China, 2020.